EURASIP Journal on Wireless Communications and Networking
a SpringerOpen Journal

RESEARCH Open Access

Searching algorithm of theodolite auto-focusing based on compound focal judgment

Chun-tong Liu, Zhen-xin He*, Ying Zhan and Hong-cai Li

Abstract

Focusing of search judgment is one of the important parts of theodolite image measurement. Traditional hill-climbing search algorithm cannot usually focus accurately due to the interference of the evaluation function of the local extremum affected by measuring environment, such as light illumination. A compound auto-focal judgment combining image definition evaluation function and modulation transfer function (MTF) auxiliary function was introduced to improve the hill-climbing method. Definition evaluation function and MTF values of images were considered to judge the search direction together. Slanted-edge method was improved to calculate the image MTF values accurately based on the auto-selection of slanted-edge area. Lastly, the principle and implementation of the improved algorithm were given. In the theodolite auto-focusing system, the system imaging effect was validated, and different initial position and circumstances were considered using the proposed searching algorithm. The experiment results of theodolite auto-focus system show that the improved hill-climbing search algorithm can effectively eliminate the local extremum disturbance and make the system search focusing accurate and reliable.

Keywords: Theodolite auto-focusing; Compound focal judgment; Modulation transfer function; Evaluation function; Hill-climbing search algorithm; Slanted-edge method

1 Introduction

There are some special functions of auto-theodolite with auto-leveling and centering, auto-axis rotation, auto-error compensation, auto-focusing, and wireless communication and signal and processing. Signal processing of images using auto-focusing is the basis for the theodolite measurement data communication and processing. With the auto-focusing technology applied universally in the digital imaging system, it has been the research focus to estimate the images definition effectively and quickly. Focusing is the important process to obtain the clear target images in the imaging system.

Compared with the traditional auto-focus technology, the auto-focus technology based on the digital image processing is attractable for its no additional hardware [1,2]. Its principles are to select the appropriate image clarity evaluation function according to the different environment, to evaluate the collected images, and then to drive the focusing mechanism to arrive at the focal position quickly and accurately according to the specific searching algorithm.

With the development of computer technology and image processing theory, the auto-focus technology based on the image processing has been continuously developed, and it is the trend of the current auto-focus technology. To improve the focus speed, Subbarao et al. put forward the defocus depth method based on the spatial domain convolution and the deconvolution transform, which is realized within the space and improved the focus speed obviously compared with the frequency domain [3]. Kehtarnavaz et al. chose the square gradient function to measure high-frequency component in the defocused image. The rule-based searching method is used to search for the focusing position of the lens, which is applied to the digital camera [4]. Gamadia et al. proposed an auto-focus method under low light, which adopted the image enhancement method to increase the contrast of the image, and the image contrast was measured by designing the focusing evaluation function [5]. For the different contrasts, an auto-focus method which is applied to television cameras was proposed [6]. Li et al. proposed an improved

* Correspondence: hezhenxin1986@126.com
Xi'an Research Institute of High Technology, Xi'an, Shaan Xi, 710025, China

Canny edge detection algorithm and improved the image edge details of the image signal and suppressed the false edge by using the wavelet transform and adaptive median filter [7]. Combining with the defocus depth method, Qi et al. proposed a focus depth method [8]. This method was used to estimate the image defocusing amount in three positions and adjust the camera directly to the focus location nearby, and then search for the best focus position with a small step. With the characteristic superiority of accuracy, this method can improve the focus speed by 37%. Han et al. put forward the Zernike's orthogonal auto-focus algorithm to avoid losing ideal characteristics of the focusing curve and being trapped in the local minima [9].

From the perspectives of the image clarity evaluation function, the focus search algorithm, and the environmental adaptability of the algorithm, there are three research focuses in auto-focus system based on the image processing. They are as follows: to improve the measurement precision of the focusing system, to shorten the time of work, and to enhance its anti-interference ability. At present, the common auto-focus searching algorithms include the hill-climbing algorithm, Fibonacci searching algorithm, and the curve fitting algorithm [10,11]. Among those algorithms, the hill-climbing algorithm with the inspired selective characteristic has been widely used to search for the best focus point in practical application. However, the hill-climbing search algorithm can only provide the relative indicators of the image sharpness, and the sharpness evaluation is vulnerable to the noise interference, which can make the result appear to the local peaks.

Based on the analysis of the three-point hill-climbing search algorithm and its shortcomings, this article puts forward the auto-focus searching algorithm based on the compound focal judgment, which adds the image modulation transfer function (MTF) with the normal focusing evaluation function to judge the focal position of the image synthetically, which enhances the reliability of the automatic focus and avoids the local peak phenomenon. Meanwhile, to improve the calculation precision of the MTF and the automation of the edge area selection, an improved calculation method of the MTF edge is adopted for the theodolite aiming system. On the basis of the principle analysis, the superiority of this algorithm will be demonstrated in the experiment. Finally, a wireless communication platform is designed experimentally.

2 The MTF calculation based on the image

2.1 The theoretical basis of MTF

MTF can be used to describe the quality of optical remote sensor and to evaluate the various aspects of imaging, and it can exist in the form of spatial frequency function at the same time, so it is more authoritative to evaluate the quality of imaging system than the method only with a certain amount of digital image, such as resolution. After years of practice, the method of evaluating the quality of the optical system using image MTF has been widely accepted and used [12].

Optical system imaging is to convert the light intensity distribution from the object plane to the image plane by Fourier analysis. The optical system can be considered as a spatial frequency filter, and the concept of MTF is brought. The object can be broken down into innumerable points, and each object point's image is corresponding to the point spread function (PSF). The image of the target is constituted by all the PSF points. Assume that the light intensity on the object plane is $o(x, y)$, and the corresponding intensity in the focal plane is $i(x', y')$. It satisfies

$$i(x', y') = \iint o(x, y)\mathrm{PSF}(x' - x, y' - y)\,dxdy \tag{1}$$

By Fourier transform, we can obtain

$$I(u, v) = O(u, v) \cdot \mathrm{OTF}(u, v) \tag{2}$$

where $O(u, v)$ and $I(u, v)$ are the Fourier transforms of $o(x, y)$ and $i(x', y')$; u and v are the frequency values along two axes' directions; $\mathrm{OTF}(u, v)$ is the Fourier transforms of $\mathrm{PSF}(x, y)$, which is called optical transfer function and it can be described as

$$\mathrm{OTF}(u, v) = \iint \mathrm{PSF}(x, y)e^{-2\pi i(ux+vy)}\,dxdy \tag{3}$$

In the condition of one dimension,

$$I(u) = O(u) \cdot \mathrm{OTF}(u) \tag{4}$$

$$\mathrm{OTF}(u) = \int \mathrm{LSF}(x)e^{-2\pi i(ux)}\,dx = \mathrm{MTF}(u) \cdot e^{-i\mathrm{PTF}(u)} \tag{5}$$

where $\mathrm{LSF}(x)$ is the line spread function of the system; $\mathrm{MTF}(u)$ is the mold of $\mathrm{OTF}(u)$; $\mathrm{PTF}(u)$ is the phase angle of $\mathrm{OTF}(u)$, which is called phase transfer function.

Assume that the object plane is based on one-dimensional sinusoidal distribution, then

$$o(x) = \alpha + b\cos(2\pi u) \tag{6}$$

According to the optical transfer characteristics, the image plane is derived as

$$i(x') = a + b\mathrm{MTF}(u)\cos\left[2\pi u x' - \mathrm{PTF}(u)\right] \tag{7}$$

From (6) and (7), we know that that the light intensity of the image is attenuated in amplitude $\mathrm{MTF}(u)$ times compared with that of the object. Therefore, MTF contains the transfer ability of the optical system and reflects the imaging quality of the system in the frequency domain comprehensively. The scene's details are reflected by the high-frequency part; the scene's gradations are reflected

by the mid-frequency part; and the scene's outline is reflected by low frequency.

2.2 The knife-edge method of MTF

As the absolute index of the system focus, the calculating method of MTF based on the image must be high-precision and operability. Knife-edge method is commonly used for MTF calculation based on the image, but it usually needs to select the edge area manually [13], which makes the calculation not be fully automated. Traditional knife-edge method requires the knife-edge line being perpendicular to the pixels, but it is impractical. Rotating a certain angle is a common method to make the knife edge vertical before calculating MTF [14], which increases the algorithm complexity and affects the calculation accuracy due to sawtooth effect caused by the image rotation. The improved knife-edge method is more reasonable and efficient to automatically select the knife-edge area. Meanwhile, the high-precision MTF calculation can be completed for the oblique edge without the image rotation. The MTF calculation steps are given as follows:

Step 1. *Selecting the knife-edge area automatically*. Detect the edge areas of the collected image to obtain the binary image. Then the binary image is detected by Hough line. From many areas in the original image, the areas with the suitable length and width are selected. The extracted effect of the knife-edge area is shown in Figure 1.

Step 2. *Building distance-gray relationship*. The gray center of each line within the edge area is fitted linearly to get the edge contour line. By calculating the vertical distance between each pixel and the edge contour line, the function between the distance and the pixel grey is obtained to depict the pixel distribution diagram. This step ensures that the algorithm can be applicable to the MTF calculation of the vertical edge and the inclined edge without image rotation.

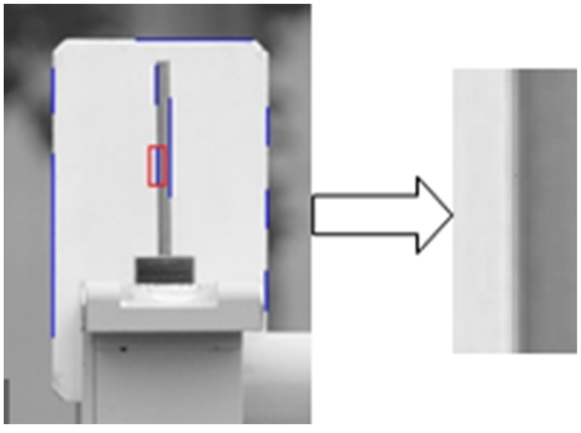

Figure 1 The extracted knife-edge area.

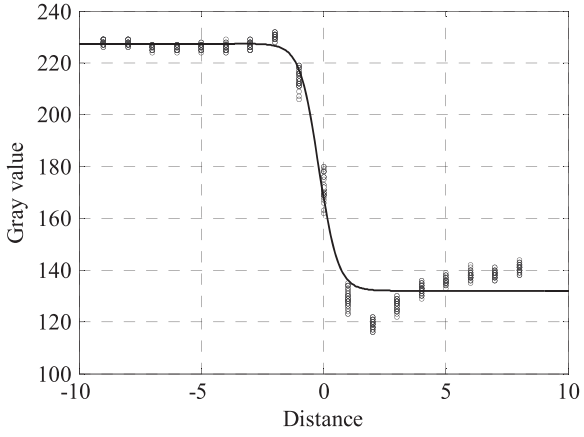

Figure 2 ESP curve.

Step 3. *Fitting the ESF curve*. Edge spread function (ESF) is the light intensity distribution function of the knife-edge image. LSF is the differential value of ESF. As the pixel distribution is easily influenced by the noise, ESF model should be constructed to fit ESF curve close to reality. The polynomial function, the composite function, and Fermi function are the common function models [15]. Due to the small knife-edge area and the small amounts of edge data, Fermi function is selected to fit ESF curve in this research, which is suitable for the small amounts of data and has the strong ability of noise suppression. Fermi function is expressed as follows:

$$f(x) = \frac{a}{1 + \exp[(x-b)/c]} \tag{8}$$

Experiments show that the linear combination of three Fermi functions can ensure the accuracy of the ESF fitting. So its common expression is

$$F(x) = \sum_{i=1}^{3} \frac{a_i}{1 + \exp[(x-b_i)/c_i]} + d \tag{9}$$

The pixel distribution data is fit by Equation 9 to get ESF curve (see Figure 2).

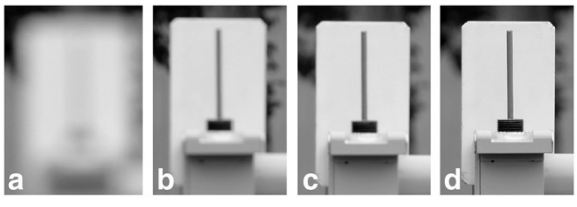

Figure 3 Image sequences of the object. (a) Defocusing. **(b)** Far-focusing. **(c)** Near-focusing. **(d)** Focusing.

Step 4. *The calculation of MTF*. ESF curve can be disposed as follows: derivate to get LSF curve; discrete LSF; make one-dimensional Fourier transform; get the modulus and make it normalized, whose result is the MTF value of response frequency. Generally, the spatial frequency needs to be normalized. The value of 1 represents the cut-off frequency, and 0.5 represents the half of the cut-off frequency, namely, Nyquist frequency. To verify the features of MTF definition, a sequence of target images from the fuzzy defocusing to the clear focusing by charge-coupled device (CCD) camera are shown in Figure 3. MTF curve of these images is shown in Figure 4.

For the image sequence, the MTF values of Figure 3a,b, c,d at the Nyquist frequency are 0.0019, 0.0049, 0.0996, and 0.0049, respectively. It proves that the greater the degree of defocus is, the more ambiguous the image will be, the faster the MTF curve will fall, and the smaller the MTF values at the Nyquist frequency will be. Therefore, the MTF values at the Nyquist frequency are available as the accessorial evaluation criterion of image resolution.

3 Design of improved auto-focusing algorithm

3.1 The choice of focusing evaluation function

According to geometrical optics theory, when the object points deviate from the object surface, the image points will become the dispersion spot. In the sides of the object plane, the discrete degree of the image is symmetrical with the object plane. Correspondingly, the focus evaluation function shall satisfy the unimodal symmetry, unbiasedness, and SNR higher features to measure whether an image is focusing. The current focusing evaluation function includes gray gradient, frequency domain, statistics, information, and wavelet, etc. [16]. The evaluation function based on image gray gradient is the most widely used definition evaluation function, which includes absolute variance function, Roberts gradient summation function, Brenner function, power function, variance function, Laplacian function, and Tenengrad function, etc. [17]. To evaluate the effect of these functions and choose a more suitable evaluation function of theodolite automatic focusing, the image sharpness evaluation contrast experiment of the benchmarking instrument is designed as follows: fixing the distance from CCD camera to the target; adjusting the focus from far to near step by step; collecting the target images and intercept 414×590 pixel section; and constituting the image sequence from fuzzy to clear and then to fuzzy again. The evaluation curves of different clarity functions are shown in Figure 5.

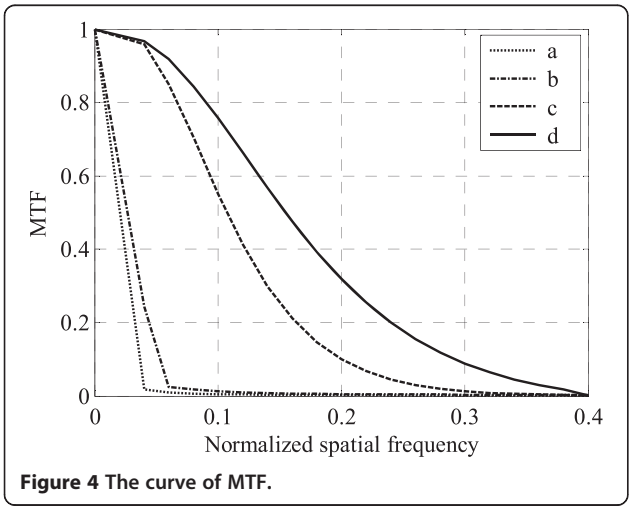

Figure 4 The curve of MTF.

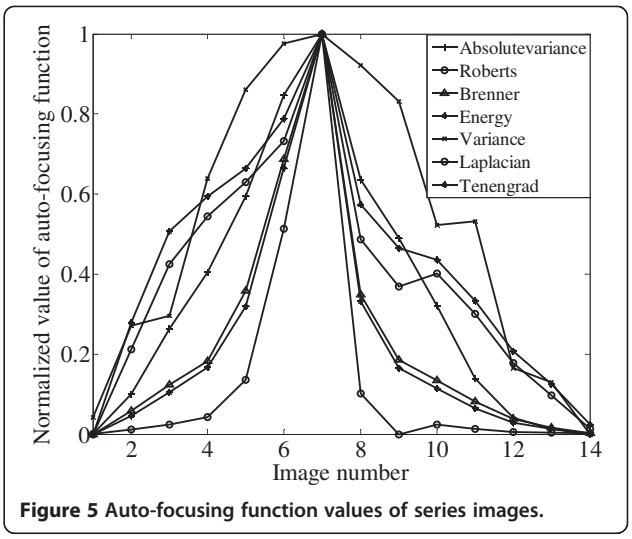

Figure 5 Auto-focusing function values of series images.

Figure 5 shows there is one and only one peak point in the curve of Brenner function or power function, and the peak width is narrower and the sensitivity is higher; but there are many peaks in other functions leading to error judgment and poor sensitivity. It takes 32 ms to evaluate a single target with Brenner function, which is shorter than other functions. Brenner function is selected as the clarity evaluation function due to its excellent comprehensive performance.

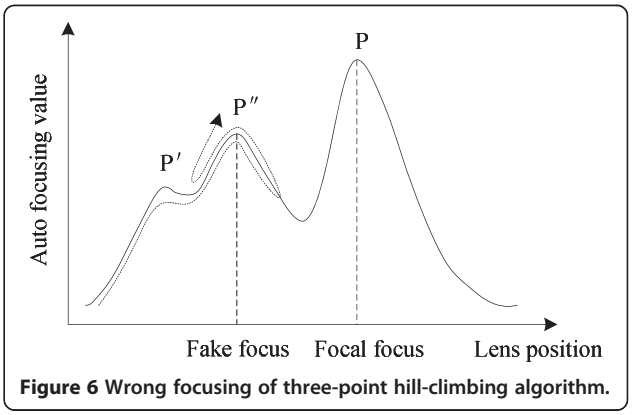

Figure 6 Wrong focusing of three-point hill-climbing algorithm.

3.2 Three-point hill-climbing search algorithm

Ordinarily, three-point hill-climbing search algorithm is improved in the present study. The hill-climbing search method is used to focus by uphill and downhill judgment using the unimodal feature of the ideal image clarity evaluation function, which is monotonously decreasing on both sides of the peak. Its searching process is as follows. The images are collected by the focusing mechanism from the initial position towards a direction. The evaluation function value is calculated, and the three consecutive images are used to judge the next action. When the evaluation function values of the three images are increasing, the images can be collected continually as the original step length and focusing direction due to the uphill state. When the evaluation function values are decreasing, it is necessary to reduce the step length and reverse the focusing direction due the downhill state. When the evaluation function values are neither increasing nor decreasing, which shows that there is the local noise or near the peak point, we can continue to collect images according to the original step length and focusing direction.

The image acquisition is highly susceptible to environmental factors, such as light, temperature, and the sensor noise. Many local peak points appear in focusing process

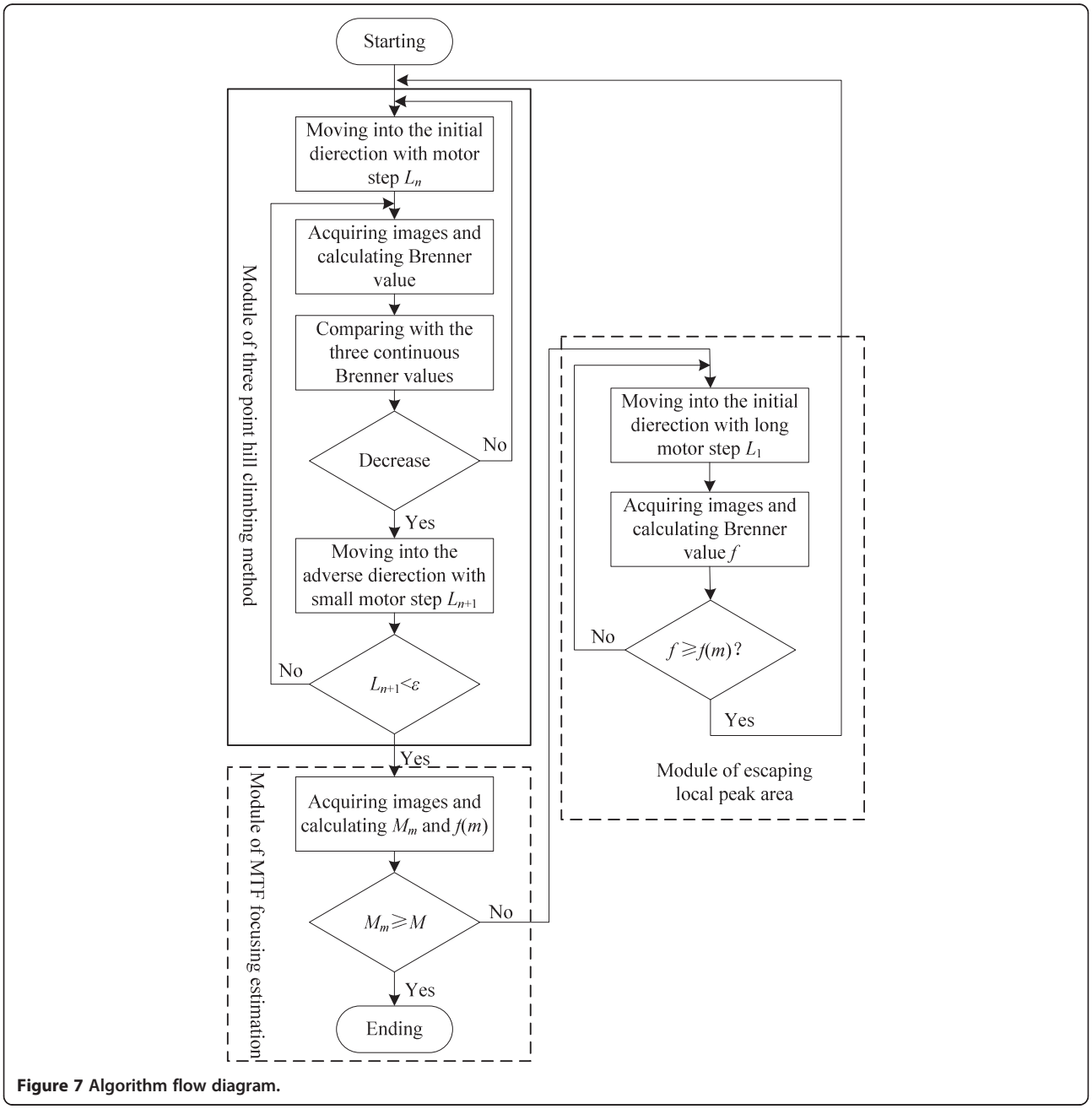

Figure 7 Algorithm flow diagram.

with the definition evaluation function. The anti-interference of the algorithm can be increased by contrasting these three consecutive evaluation function values. But the three-point hill-climbing search method is usually applied to the a few local peaks situation and the small range of the peak points. For the large local peaks scope, the three-point hill-climbing method still can appear as the focusing error to search the local peak point P" in Figure 6.

3.3 The principle and implementation of the improved focusing algorithm

When the focusing mechanism stops at P" point, it can avoid the focusing error if there is another evaluation function to further judge whether this point is the focal position. The MTF value of the collected image is calculated, which is compared with the MTF values of the pre-arranged focal images, and the judgment of the focusing error is completed. The MTF values of the optical system do not vary with the collected image changes [18], so the MTF values at the Nyquist frequency can be gotten via testing the focusing optical system in advance. When a focus process is finished by using the three-point hill-climbing method to stop at a peak point, the MTF values of the collected images at Nyquist frequency are calculated. When this value is less than the setting standard, it shows that the location is a local peak, not the real focus, so the focusing needs to be continued. When the MTF value at Nyquist frequency is greater than or equal to the setting standard, it shows that the focusing is correct. It is the compound focusing searching strategy, combining the three-point hill-climbing method and MTF auxiliary focal judgment, which avoids focus errors effectively and ensures fast searching. The improved algorithm process is shown in Figure 7 as follows:

Step 1. MTF values of the collected images at the Nyquist frequency is $\mathrm{MTF}_{\mathrm{Nyquist}}$, and $M = \alpha\mathrm{MTF}_{\mathrm{Nyquist}}$ $(0.90 \le \alpha \le 1)$ is stored as the focal judgment standard.

Step 2. Focusing mechanism operates from the nearest position (or the farthest) with a large step $L_{\mathrm{n}}(n = 1,2,3\ldots,$ the nth step focal action). Brenner evaluation function values of the collected images are calculated. Comparing the evaluation function values of the three images, if three evaluation function values are increasing, focusing is continued along the original direction with the step length L_{n}; if decreasing, focusing is carried out along the opposite direction with the smaller the step length $L_{\mathrm{n}+1} = \beta L_{\mathrm{n}}$ $(0 < \beta < 1;\ \beta$ can be determined by the experiment); If equal, focusing is continued along the original direction with the original step length. The above process is ending until $L_{\mathrm{n}} < \varepsilon$ (ε is the setting accuracy).

Step 3. When the focusing mechanism stops, the images are collected and the evaluation function values $f(m)(m = 1,2,3\ldots,$ show it had detected the peak point m P_{m}) and MTF values M_{m} at the Nyquist frequency are calculated, If $M_{\mathrm{m}} \ge M$, the place is the focus position, and then the focusing process is completed. If $M_{\mathrm{m}} < M$, the place is the local peak point, and then the focusing mechanism continues to focus with the step length L_1 according to the initial state. If the focus function value in the new location is greater than the $\max\{f(1), f(2)\ldots f(m)\}(m = 1,2,3\ldots)$, it has been out of the scope of local peaks, and then focusing mechanism continues along the opposite direction (the direction of the focal length decreasing); otherwise, it moves along the direction of the focal length increasingly.

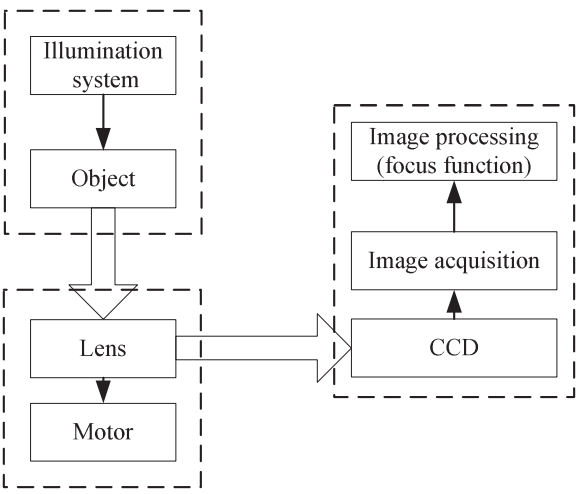

Figure 8 The schematic of experimental system.

Step 4. Follow step 2 and carry out focusing. When the maximum is detected, the focusing mechanism is stopped. The movement direction and step length are judged as is described in step 3.

Step 5. Repeat steps 2, 3, and 4 until the $M_{\mathrm{m}} \ge M$. The whole focusing process is completed.

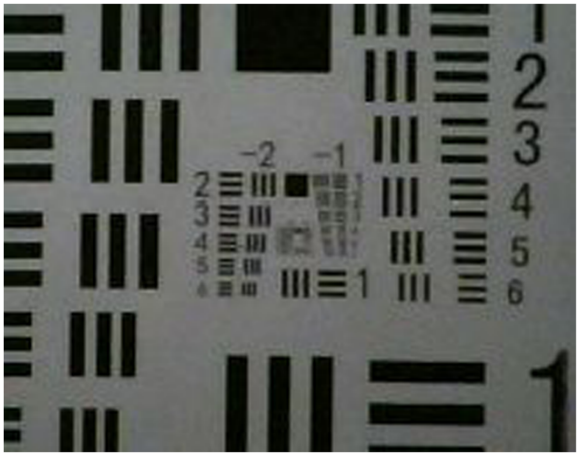
Figure 9 Image of resolution checker.

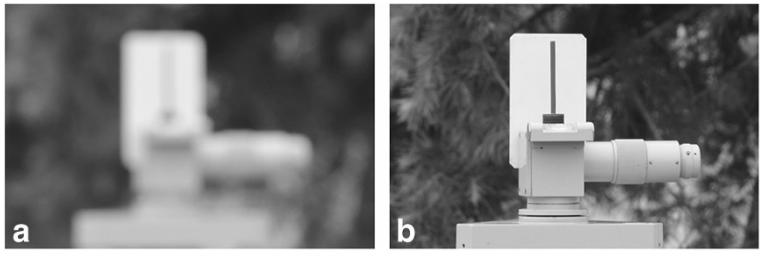

Figure 10 Benchmarking images contrast between before and after auto-focusing. (a) Defocusing image. **(b)** Focusing image.

4 Automatic focusing experiments

Automatic focusing experiments are carried out to verify the effectiveness of the designed searching algorithm and the experiment platform consists of industrial CCD camera MV-300UC-D (2,048 × 2,048 pixels), the modification of J2 electronic theodolite (the adding focus hand wheel is driven by RM2414S focusing stepper motor) and the computer image processing system. The schematic of experimental system is shown in Figure 8.

4.1 Resolution board imaging experiment of automatic focusing system

Resolution board is one of the common tools in the photoelectric imaging system evaluation. The resolution board image using the proposed method is shown in Figure 9.

From Figure 9, the imaging effect of auto-focusing system is quite good. The system can provide an experiment platform for the algorithm.

4.2 The contrast experiment of the focusing performance with different initial positions

Experiment method is carried out as follows: (1) install the benchmark gauge in the place, about 10 m away from the theodolite, regulate theodolite manually to make it aim at the benchmark, calculate the MTF value to gain $MTF_{Nyquist}$, and select the appropriate value of α; (2) regulate the focusing hand wheel to the close focal position. Four group experiments are designed, and the original positions of the focusing hand wheel are set at 0°, 2°, 4°, and 6° respectively. The before and after automatic focus images of group 1 are compared and analyzed. Figure 10 shows the contrast images.

The results show the focusing effect is significant, and the clear images can satisfy the target recognition and measurement requirements of the system. The prism replaces the benchmarking by using the same method and carrying out steps 1 and 2. The contrasted prism images before and after auto-focusing are shown in Figure 11.

From Figures 10 and 11, the collected images after focusing are both clear for the different aiming targets, and the method has the strong adjustability for the targets.

Brenner function value curves in benchmarking focusing of the four groups are shown in Figure 12.

The motor starting positions of the four group experiments are different, but the focus results are consistent at about 84° position. The clear focal image should have greater contour grayscale differences than fuzzy image, and the difference of their Brenner function and MTF value is bigger from the experiment, so the standard derivation of the evaluation function between the images can be taken as the effective focusing evaluation tool. The focusing results of four experiments with focal image normalization Brenner function values, Nyquist frequency MTF, average values of MTF, and standard deviation are shown in Table 1.

It is known that the standard deviation is small, which shows that the four focusing results are very similar. The result is satisfying from the focal images of four group experiments. The standard deviation of the normalized

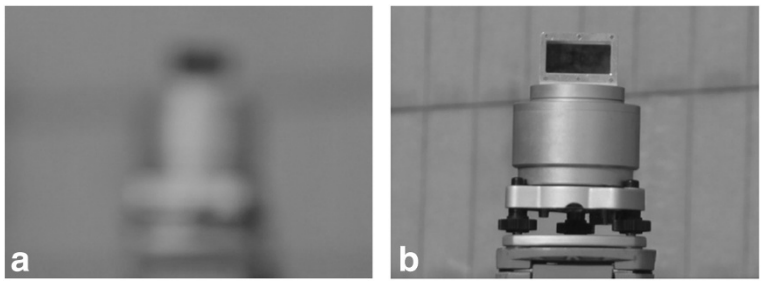

Figure 11 Prism images contrast between before and after auto-focusing. (a) Defocusing image. **(b)** Focusing image.

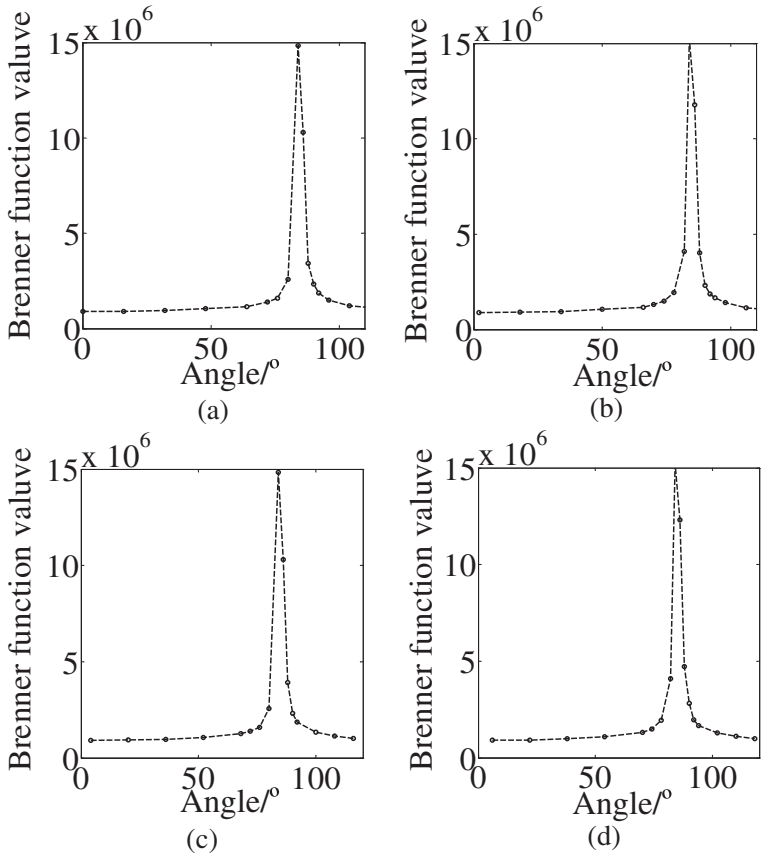

Figure 12 Brenner value in the process of focusing. (a) Defocusing. **(b)** Far-focusing. **(c)** Near-focusing. **(d)** Focusing.

Brenner value and the MTF values shows that the algorithm can be used to realize automatic focus effectively, and it is repeatable and stable under the different defocusing levels. The total focusing time mainly includes image acquisition and processing, the control signal transmission, and the motor running, and delay. Among them, the motor running time is the main factor that affects the system focusing time. To prevent conflict between signals, each running needs 0.2 s delay; the adjustment steps of the machine are related to the initial defocusing state of the system, which may also affect focusing time. In the focusing experiment, the adjustment steps of focus motor are about 21 to 25 s, and the average time of four group experiments is 12 s, which satisfies the time requirements of the theodolite auto-focusing.

Table 1 The focusing results

List	1	2	3	4	AV	SD
Brenner	0.9883	0.9994	0.9963	1.00	0.9960	0.0093
$MTF_{Nyquist}$	0.1364	0.1405	0.1389	0.1416	0.1394	0.0039

AV, average; SD, standard deviation.

4.3 The searching algorithm experiment with the environment change

The above four experiments are conducted in a relatively ideal environment, so there is no obvious local peak appearing in Brenner function value curve, which will not affect the search judgment of the hill-climbing method. To further verify the reliability of the algorithm, the

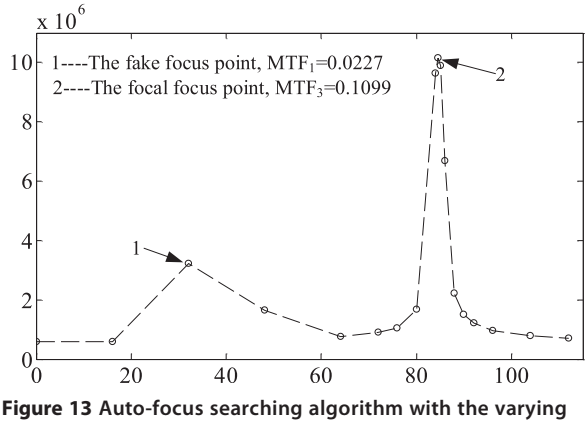

Figure 13 Auto-focus searching algorithm with the varying environment.

experiment method is the same as that in Section 3.2. The original position of the focusing hand wheel is still at 0°, while the focusing environment changes. By the LX-1010B-type digital luminometer, the instrument benchmarking of the surrounding light intensity is measured. The average light intensity before and after lighting is 5,500 lx into 10,400 lx before and after lighting. The experiment data point is sampled after focusing, and the focus position and Brenner evaluation function curve are shown in Figure 13.

Figure 13 shows that the Brenner function value is small when the defocusing amount of the image is bigger. When it is close to the focal state, the Brenner function value changes rapidly. After a short lighting operation of instrument benchmarking, the Brenner function values go up and down suddenly to form a wave crest. According to the ordinary mountain climbing algorithm or three-point hill-climbing algorithm, the focus process will eventually stop near the crest, at point 1. However, this position is not the focal position, and it will cause a false focusing operation. Based on the proposed compound focusing judgment algorithm, the MTF values of the real-time image are calculated when the wave occurs, and then they are compared with the MTF reference values of the stored images. By debugging in advance, the reference MTF value is 0.1148, and the fault tolerance rate is 10%. We know that the MTF value of 1 point is out of tolerance, which can be considered as the false focusing wave. The focusing motor is operated to make it focus on position 2 (84.5°), which is consistent with the former four focusing results. Compared with the previous mentioned four focusing experiments, the Brenner function values of the images and the MTF values happen to change accordingly as the focusing environment changes. Image MTF reference values are obtained by the artificial debugging before each experiment and the MTF modeling based on the environment factors.

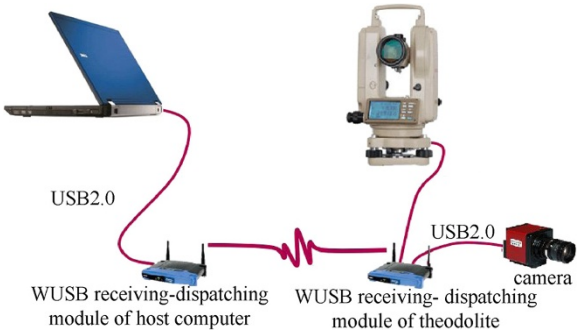

Figure 15 WUSB data communication system between theodolite and PC.

The experimental analysis shows that this algorithm has the strong anti-interference ability in the actual application, which can improve the auto-focusing reliability of theodolite and that of other photoelectric equipments in a complex environment.

4.4 Reliability experiment of the proposed MTF estimation method

To validate the reliability of the proposed MTF estimation method, two knife-edge target images and three different selected sites in the theodolite auto-focusing system with different contrasts, signal-to-noise ratios, and incline angles are shown in Figure 14a. MTF estimation precision results are obtained as shown in Figure 14b.

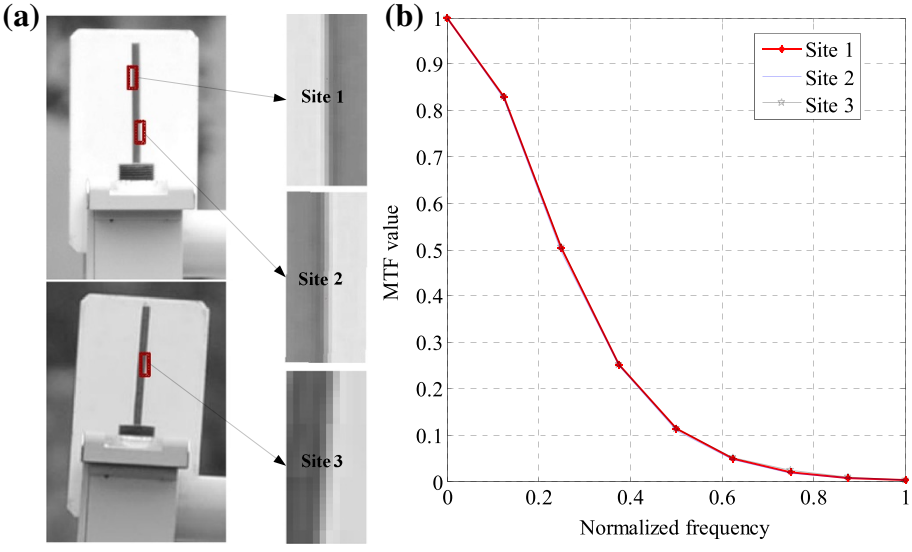

Figure 14 MTF estimation experiment with theodolite pole image. (a) Three knife-edge sites. **(b)** Estimation results.

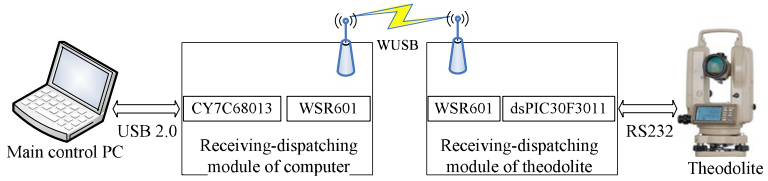

Figure 16 WUSB hardware system scheme.

From Figure 14, Nyquist frequency values of three sites are 0.124, 0.117, and 0.111, respectively. Comparatively speaking, the maximum absolute error and SD are both minimal, which are about 0.013 and 0.00534. The MTF of site 1 and site 2 is bigger than that of site 3. Considering incline angles, contrasts, and target random noise, the major reason of the smaller MTF of site 3 is that it has lower contrasts and bigger incline angles. Furthermore, the low contrast declines the whole image quality to make knife-edge areas' details illegible. Based on the analysis in Section 3, the MTF precision gets lower with the bigger incline angles, and the experiment results prove the correctness of knife-edge method analysis in this paper. The three influence factors' principle of MTF precision estimation is believable.

4.5 Wireless communication platform design

To solve the problem of the theodolite portability and operation, wireless USB (WUSB) images data communication system is used for auto-theodolite and PC. The sketch map is given in Figure 15.

The WUSB transmission system includes four function units: wireless unit, link control unit, link management, and software function package. Microcontroller CY7C68013 with USB interface from Cypress Corporation (Dubai, United Arab Emirates) and WUSB single emission chip WSR601 from Wisair Corporation (Tel Aviv, Israel) are combined to design the WUSB receiving-dispatching module circuit hardware of the host computer. Meanwhile, the 16-b SCM dsPIC30F3011 from Microchip Corporation (Chandler, AZ, USA) and WSR601 are used to design the WUSB receiving-dispatching module circuit hardware of the theodolite. The WUSB hardware system scheme is given in Figure 16.

5 Conclusions

The searching algorithm of theodolite auto-focusing based on compound focal judgment can eliminate disturber effectively, avoid the local undulation of the focusing estimation function, and improve the auto-focusing reliability by combining the common images definition estimation function and MTF value of images. The improved knife-edge method can solve the MTF value of images accurately and automatically to provide the focusing reference. Meanwhile, the proposed searching algorithm supports the theodolite auto-focusing based on the image processing in the theory. The experiment results show that the proposed algorithm can satisfy the theodolite auto-focusing requirements from the perspectives of the focus precision, the focus time, and the focus reliability. The proposed algorithm can be also adopted in other photoelectricity equipments.

Competing interests
The authors declare that they have no competing interests.

Received: 16 June 2014 Accepted: 30 June 2014
Published: 9 July 2014

References

1. M Moscaritolo, H Jampel, F Knezevich, R Zeimer, An image based auto-focusing algorithm for digital fundus photography. Med. Imag. **28**(11), 1703–1707 (2009)
2. C Florea, L Florea, A parametric non-linear algorithm for contrast based auto-focus, in *International Conference on Intelligent Computer Communication and Processing* (Cluj-Napoca, 2011), pp. 267–271
3. C Chen, *Study on strategy of long-range rapid auto-focusing for image-based three dimension measurement system, Thesis* (Shanghai Jiao Tong University, Shanghai, 2009)
4. N Kehtarnavaz, HJ Oh, Development and real-time implementation of a rule-based auto-focus algorithm. Real-Time Imag. **9**, 197–203 (2003)
5. M Gamadia, N Kehtarnavaz, K Roberts-Hoffman, Low-light auto-focus enhancement for digital and cell-phone camera image pipelines. IEEE Trans. Consum. Electron. **53**(2), 249–257 (2007)
6. F Hu, Y Chang, Y Ma, G Zhao, Development of video automatic focus method. Acta. Photonica. Sinica. **39**(10), 1901–1906 (2010)
7. J Li, Y Ma, F Zhao, L Guo, A novel arithmetic of image edge detection of Canny operator. Acta. Photonica. Sinica. **40**(1), 50–54 (2011)
8. Q Li, H Feng, Z Xu, Method of improving autofocus speed based on defocus estimation. J. Optoelectronics Laser **16**(7), 850–853 (2005)
9. R Han, J Wang, K Nie, Y Liu, Adaptive autofocus technique under different contrast. Acta. Photonica. Sinica. **41**(2), 222–227 (2011)
10. X Xie, J Zhou, Q Wu, An adaptive autofocus method using no-reference structural sharpness. Opto-Electron. Eng. **38**(2), 84–89 (2011)
11. T Hu, S Chen, G Liu, Z Pu, Algorithm of rapid auto-focusing with a long-range. J. Optoelectronics Laser **17**(4), 474–467 (2006)
12. J Liao, X Gao, W Liang, Dynamic MTF analysis and research for aerial camera. Acta. Photonica. Sinica. **44**(5), 679–683 (2011)
13. T Li, *Research on modulation transfer function calculation and remote sensing image restoration based on slanted-edge method, Dissertation* (Zhejiang University, Hangzhou, 2011)
14. Z Lu, *The automatic image-based real-time focusing research in pushbroom remote sensing camera, Dissertation* (Changchun Institute of Optics, Fine Mechanics and Physics, Chinese Academy of Science, Changchun, 2012)
15. Y Wang, J Mao, A simple method for calculating Fermi function with MATLAB and numerical approximation. Infrared **29**(8), 34–36 (2008)

16. H Shi, Y Shi, S Yang, Evaluation and selection of estimating function for auto-focus system of optical microscope. J. Comput.-Aided Des. Comput. Graph. **25**(2), 235–240 (2013)
17. J Wang, H Chen, G Zhou, T An, An improved Brenner algorithm for image definition criterion. Acta. Photonica. Sinica. **41**(7), 855–858 (2012)
18. J Liu, M Gao, *Optical design* (National Defense Industry, Beijing, 2012)

doi:10.1186/1687-1499-2014-110
Cite this article as: Liu *et al.*: Searching algorithm of theodolite auto-focusing based on compound focal judgment. *EURASIP Journal on Wireless Communications and Networking* 2014 **2014**:110.